CONF-850507--19

UCRL-92666
PREPRINT

MEASUREMENTS AND CALCULATIONS OF NEUTRON SCATTERING ANGULAR DISTRIBUTIONS OVER A WIDE MASS AND ENERGY RANGE

Luisa F. Hansen

University of California
Lawrence Livermore National Laboratory
Livermore, CA 94550

This paper was prepared for submittal to
The International Conference on Nuclear
Data for Basic and Applied Science
Santa Fe, NM USA
May 13-17, 1985

May 1985

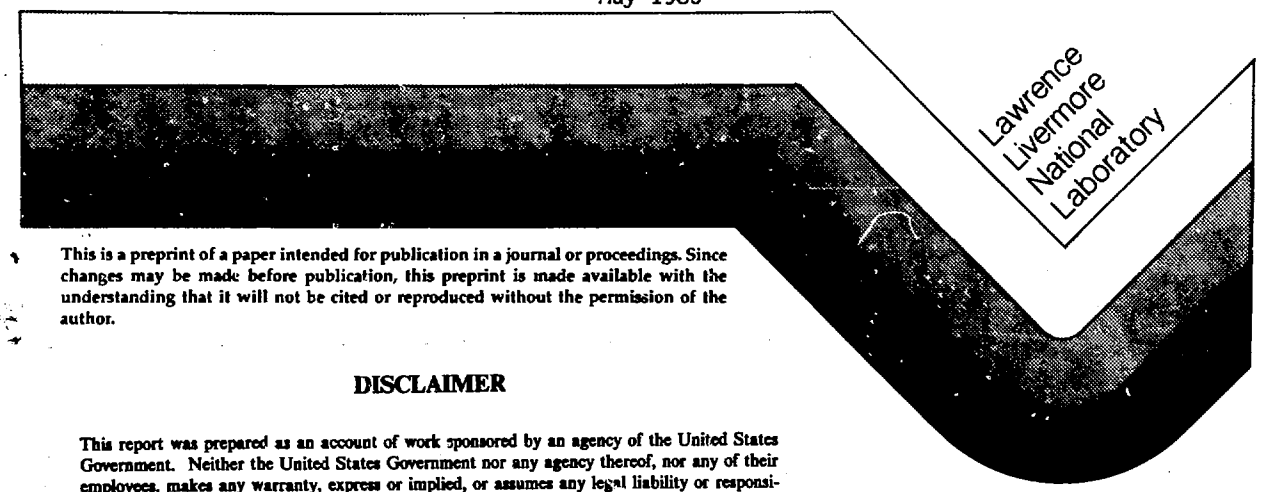

DISCLAIMER

L. F. HANSEN

UCRL--92666

DE85 012912

MEASUREMENTS AND CALCULATIONS OF NEUTRON SCATTERING ANGULAR DISTRIBUTIONS OVER A WIDE MASS AND ENERGY RANGE*

LUISA F. HANSEN
LLNL, Livermore, CA 94550, U.S.A.

Abstract Neutron elastic and inelastic differential cross sections for targets between ^{9}Be and ^{239}Pu at energies, E > 14 MeV have been measured using the Livermore and Ohio University neutron time-of-flight facilities. We review here the data and the analyses based on two local microscopic optical potentials: that of Jeukenne, Lejeune and Mahaux, and that of Brieva and Rook. The results are also compared with calculations using global potentials. Coupled channel formalism has been used in the analysis of targets with strong deformations, such as Be, C, Ta, and actinides. The value of the microscopic optical potentials as a tool to predict elastic and inelastic neutron cross sections over a wide mass and energy range is discussed. The need for neutron measurements up to higher energies and their analysis in conjuction with (p,p) and charge exchange (p,n) data is addressed.

INTRODUCTION

The differential neutron scattering measurements to be reviewed have been carried out at LLNL and Ohio University in the last three years. The objective was to generate a consistent set of neutron data over a wide mass and energy range to test two local microscopic optical potentials (MOP) due to Jeukenne, Lejeune, and Mahaux (LJM)[1], and Brieva and Rook (BR)[2]. To carry out a systematic test of these potentials over a wide mass range, the culations were compared with the elastic angular distributions at 14.6 MeV for targets from Be to Bi. The energy range considered here is from 8 to 26 MeV for selected targets. Although there exists a large body of measurements at 14 MeV[3], the comparison would have been less effective given the large

differences in experimental conditions and analysis of the data (beam energy, resolution, detector efficiency, multi-scattering corrections, etc.). An important result from the above comparison is that only two normalizing parameters, λ_V and λ_W for the real and imaginary potentials respectively, have been used in the calculations, and the agreement obtained with the measurements is qualitatively the same or better than that obtained with global potentials[4] optimized for the mass region. For the actinide targets ^{232}Th, ^{238}U and ^{239}Pu characterized by strong deformations, the measurements were compared with the results of a semi-microscopic coupled channel (CC) calculation[5] using the JLM potential and deformed neutron density distributions. Calculations carried out with deformed global optical potentials[6] for the actinide region (En < 15 MeV) gave results comparable to those obtained with the JLM potential. For the lighter deformed nuclei, Be, C and Ta, the agreement between the calculated and measured angular distributions improved noticeably by carrying CC calculations[7].

The JLM and BR microscopic OP have also been tested as function of energy (7-65 MeV) in the analysis[8-10] of elastic and inelastic differential cross sections for proton (20-65 MeV) and neutron scattering (8-26MeV). Dietrich et al.[8] have shown that in order to get consistency between neutron and proton scattering, the microscopic potentials for both neutron and proton scattering must be calculated from an asymptotic energy E, instead of at a value shifted by the Coulomb potential ($E-V_{Coul}$). In the local MOP there exists in addition to the intrinsic E-dependence, a second dependence on the energy of the projectile. This results from the local-momentum approximation for the exchange term in the OP (energy conservation is used to substitute the momentum dependence: $p^2/2m = E-Vnuc-V_{Coul}$) accounts almost completely for the energy dependence of the real term in the MOP and gives rise to the term $E-V_{Coul}$, found in global OP.

In the comparisons with the JLM and BR microscopic potentials it has been found that the JLM microscopic optical potential does systematically better than the BR potential as function of mass and energy.

In addition to microscopic and global neutron optical model potentials (OMP) used in the analysis of neutron scattering data, the Lane formulation[11] of the OMP (from the charge-independent two body force) allows the extraction of neutron potentials from proton data[12]. It has been shown[13] that the Lane formalism generalized to include channel coupling effects becomes a powerful tool which can be used to calculate neutron differential cross sections for

heavy nuclei, including the actinide region. This is illustrated in the calculations of the neutron scattering from ^{232}Th, ^{238}U and ^{239}Pu at 14.1 MeV by solving the Lane CC equations for the proton and neutron channels. A deformed OP obtained from proton scattering[14] at 35 MeV from these nuclei, and the isovector potential obtained from (p,n) data[13], were used in the calculations. These results compare well with those obtained with the deformed microscopic and global OP.

MEASUREMENTS

The angular distributions for the elastic scattering of 14.6 MeV neutrons from ^{9}Be, C, ^{27}Al, Fe, ^{59}Co ^{89}Y, ^{93}Nb, In, ^{140}Ce, ^{181}Ta, ^{197}Au, ^{208}Pb, ^{209}Bi, ^{232}Th, ^{238}U, and ^{239}Pu were measured using the LLNL time-of-flight (TOF) facility. The 14.6 neutrons were produced by the $^{2}H(d,n)^{3}He$ reaction at 0° using the 12 MeV incident deuteron beam from the LLNL tandem electrostatic accelerator. The scattered neutrons were detected using NE213 liquid scintillation detectors with a threshhold at≈5.4 MeV

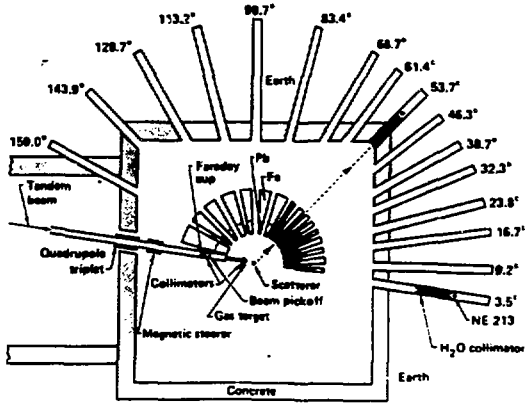

FIGURE 1 Schematic representation of the Livermore time-of-flight facility.

and pulse shape discrimination to reduce the gamma-ray background. The TOF facility allows simultaneous measurements for 16 angles in the angular range 3.5° to 159°. The elastic differential cross sections were measured in the angular range 9.2° to 159° with a 10.75 m flight path for all the detectors. The 3.5° detector turned off during the scattering run is used to measure the incident flux on the scatterer. Fig. 1 shows a schematic view of the TOF facility, details on the experimental technique can be found in Ref. 3.

MICROSCOPIC OPTICAL POTENTIALS

The microscopic optical potentials (MOP) contain the central and spin-orbit potentials which include the direct and exchange terms. The central potentials are calculated by folding integrals of an effective interaction, g(r), between the projectile and target nucleons with the nuclear density. The exchange terms are calculated by carrying a suitable local momentum approximation of g(r).

$$U(r_1) = \int \rho(r_2) g(r) d^3 r_2 \qquad (1)$$

r_1 and r_2 refer to the projectile and target nucleons respectively; $r = (r_1 + r_2)/2$ is a reasonable, although not rigorously tested "local density approximation". The nuclear density, $\rho(r)$ for neutron scattering was assumed to be proportional to the proton density obtained from electron scattering. For heavier nuclei ($A > 100$), calculations were done also assuming a "neutron skin" with about 2.6% increase in the neutron rms radius over the one of the proton, but the results were not sensitively different for the energy of these measurements. The effective interaction g(r) is complex, radial, density and energy dependent, $g[r,\rho(r),E]$. Brieva-Rook[2] (BR) start from the Hamada-Johnston free nucleon-nucleon interaction to calculate the energy and density dependent t matrix, $t(r,\rho,E)$, from which the optical potential in a finite nucleus is calculated by folding integrals (Eq. 1). Jeukenne, Lejeune, and Mahaux[1] (JLM) calculation starts from the Reid's hard core nucleon-nucleon interaction and yields directly the energy and density dependent optical potential in infinite nuclear matter, $U(\rho,E)$. The potential for a finite nucleus is then calculated using a local density approximation. In both the JLM and BR potentials, only the central direct and exchange potentials were calculated as prescribed. The spin-orbit (SO) potential was calculated[9] using the effective interaction from the Elliott spin-orbit version of the M3Y force[15], which is real and independent of energy and density.

Test Over Mass Range. The predictions of the MOP were compared with the elastic angular distribution data at 14.6 MeV by multiplying the real and imaginary terms of the central potential by normalizing constants, λ_V and λ_W, respectively. These parameters were adjusted by least squares for an optimal fit to the data. In Figs. 2-4 are shown the comparisons between the MOP after normalization and the measurements. The overall agreement is reasonable for both potentials, with the JLM potential giving a better representation of the data over the entire mass range.

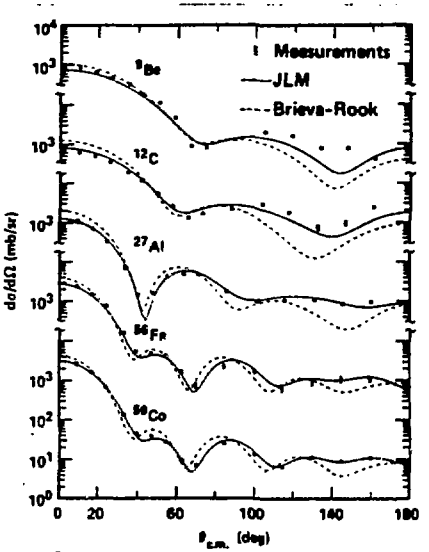

FIG. 2 Measurements of (n,n_o) at 14.6 MeV and calculations with the JLM(-) and BR(---) MOP.

The values of the normalizing parameters, λ_V and λ_W for each of the target nuclei are shown in Fig. 5.

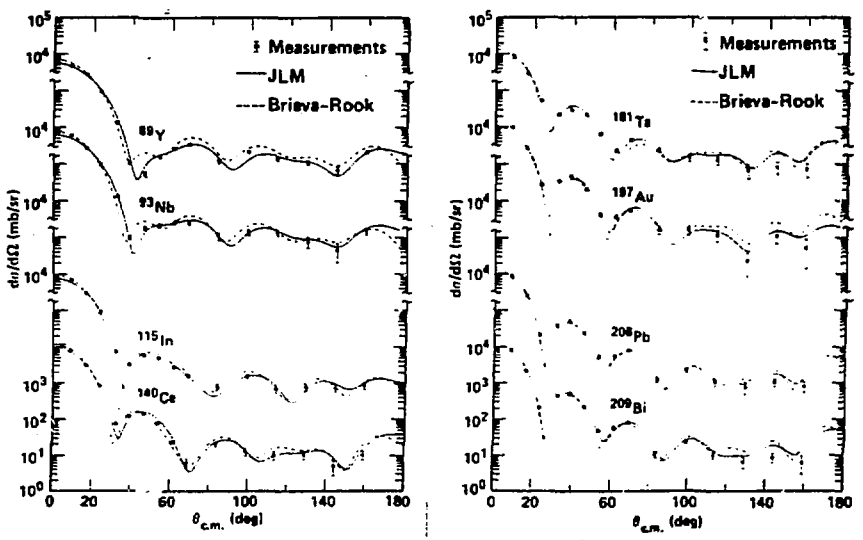

FIG. 3, 4 Measurements of (n,n_o) at 14.6 MeV and calculations with the JLM(-) and BR(---) MOP.

For the real central potential, the value of λ_V is close to unity for all the values of A in both the BR and JLM potentials. The normalizing parameters λ_W show larger fluctuations than λ_V for both MOP, although they have a definite decreasing trend with A value.

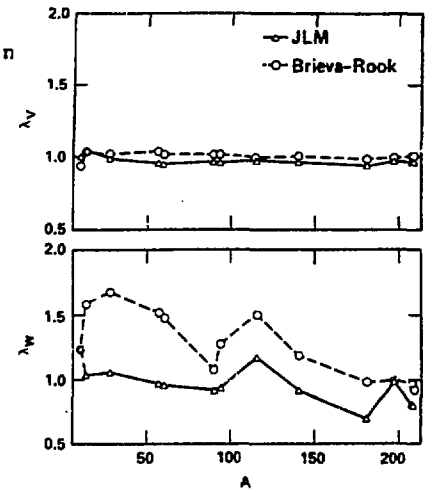

FIG. 5 Values of the parameters λ_V and λ_W from fits to (n,n_o) at 14.6 MeV over mass range: JLM(Δ), BR(o).

The quality of the fits obtained with the MOP (Figs. 2-4) was compared with calculations carried out with the global OP of Rapaport et al.[4] optimized to fit neutron data in the energy range E < 15 MeV. Following the same normalizing procedure used with the MOP, the fits to the data were obtained by a least squares fitting of the real and imaginary potentials V_R and W_D. The ratios between the values of these potentials after the search and their initial values prescribed by the global set[4] are called λ_V and λ_W in analogy with the microscopic calculations. The agreement between the calculations with the global potential and the data are close to the predictions obtained with the JLM potential. The curves have not been plotted in Figs. 2-4, but the values obtained for χ^2/N and the normalization parameters λ_V and λ_W are listed in Table I together with the values from the JLM microscopic OP. The values of χ^2/N for the BR potential were factors of 2 and 3 larger than those obtained with the JLM potential. For the values of λ_V and λ_W see Fig. 5.

TABLE I Values of χ^2/N and the normalization parameters λ_V and λ_W for the neutron angular distributions at 14.6 MeV with the JLM microscopic OP and Rapaport et al. global OP.

	JLM			Rapaport et al.	
Target	χ^2/N	λ_V	λ_W	χ^2/N	λ_V	λ_W
Be	29.4	1.00	1.25	40.2	0.96	0.83
C	14.1	1.04	1.04	32.5	0.96	0.83
Al	6.3	0.99	1.06	12.0	0.96	0.72
Fe	3.9	0.96	0.97	4.0	1.00	0.78
Co	2.6	0.95	0.96	6.7	0.98	0.82
Y	5.5	0.97	0.92	8.0	1.00	0.84
Nb	2.0	0.96	0.94	2.2	0.98	0.96
In	7.2	0.98	1.18	7.6	1.00	1.07
Ce	7.6	0.97	0.92	7.5	1.02	0.84
Ta	6.8	0.94	0.70	6.5	0.99	0.87
Au	7.6	0.98	1.00	3.1	0.99	0.92
Pb	4.0	0.97	0.81	2.9	1.00	0.84
Bi	8.2	0.97	0.80	6.4	1.00	0.82

Test Over Energy Range. Dietrich et al.[8-10] have tested the BR and JLM potentials over the energy range 7-65 MeV for light[10] (C, O, N,Al) and heavy[7,8](Fe and Pb) nuclei. They have carried out calculations for both protons and neutrons in order to study transition densities, Coulomb corrections and the isovector term [(p,n) reactions] of the effective interaction. The measured neutron elastic angular distributions for ^{54}Fe between 8 and 26 MeV are compared[8] in Fig. 6 with calculations done with the microscopic optical potentials of BR and JLM. As in the comparisons shown in Figs. 2-4 for the 14.6 MeV data, JLM potential gives a better fit over the whole energy range. The differences between the two calculations in both mass and energy range tests are more pronounced at the forward angles, where the BR calculation over-predict the differential cross sections, and in the behavior of the angular distributions at larger angles ($\theta >$ 100). These differences have been traced[9] to the different shapes of the real potential which, for the JLM potential, is close to a Wood-Saxon shape while for the BR potential shows a non-smooth behavior (a "bump") in the region of the nuclear surface. For lighter nuclei where the surface region becomes a larger fraction of the nuclear volume, the BR potential overestimates[3] the total cross sections by factors of 10 to 20% for A values between 9 and 100.

The values of the normalizing parameters λ_V and λ_W for the ^{54}Fe calculations are shown in Fig. 7.

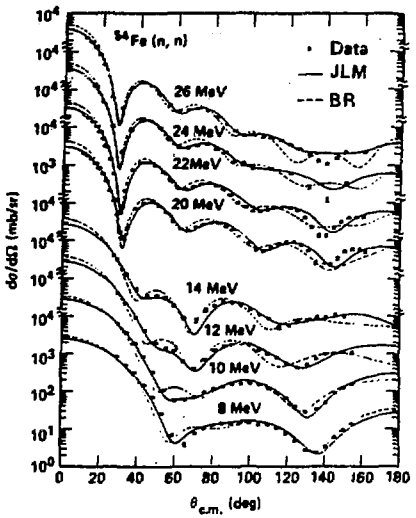

FIG. 6 Measurements and calculations of ^{54}FE(n,n_o) over the energy range 8-26 MeV.

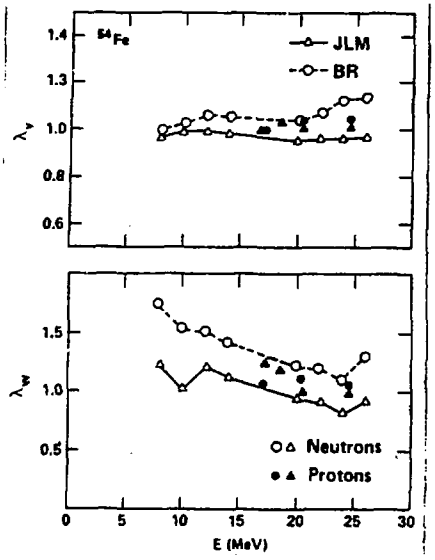

FIG. 7 Values of parameters λ_V and λ_W from fits to ^{54}Fe(n,n_o), open Δ (JLM) and o (BR); and fits to (p,p_o), dark ▲ and ●.

As discussed earlier for the 14.6 MeV data, the value of λ_V is very close to unity for both potentials. In the BR calculation, the values of the normalization constants for the imaginary potential are larger than the JLM values for energies below 20 MeV, with an increasing trend forward lower energies. The values of the parameters obtained from fitting proton angular distributions[9] with these two MOP are also shown in Fig. 7. They are in reasonable agreement with the values obtained from the neutron scattering fits.

DEFORMED NUCLEI AND COUPLED CHANNEL CALCULATIONS

Among the targets included in the study of neutron elastic scattering at 14.6 MeV, Be, C and Ta are characterized by strong deformations ($0.2 < \beta_2 < 1.2$) In the calculations done with the BR and JLM microscopic potentials[1,2] (Figs. 2-4), or with the global potential of Rapaport *et al.*[4] (Table I), these targets were taken to be spherical nuclei. To study the effects of the deformation in the calculations of the differential scattering cross sections, these were calculated using CC formalism and deformed OP.

The test[7] was carried out only for global OP and the code[16] ECIS79 was used in the CC calculations. These included in addition to the ground state (GS), the first two low excited levels which are members of the GS rotational band. The Legendre multi-pole expansion of V_R and W_D included terms up to $l = 6$ for all calculations (for details on these calculations see Ref. 7). Fig. 8 shows the comparison between the measurements and the angular distributions calculated with: a) the global spherical OP (dashed lines) whose results are listed in Table I, and b) a deformed OP. For Be and C the deformed OP of Meigooni et al.[17] from neutron scattering from C over a wide energy range was used in the CC calculations (solid lines). This OP reproduced also quite well the neutron elastic and inelastic (4.43 MeV) angular distributions measured[7] at energies between 13.6-14.8 MeV. For Ta, the CC calculations were carried using the spherical OP of Rapaport et al.[4] corrected for coupling. The solid curve corresponds to the sum of the calculated angular distributions for the GS and 0.136 and 0.301 MeV excited levels, since the resolution of the measurements (∿ 300 keV)did not resolve them. Fig. 8 shows that the quality of the fits was improved by the inclusion of coupling among the GS and excited levels.

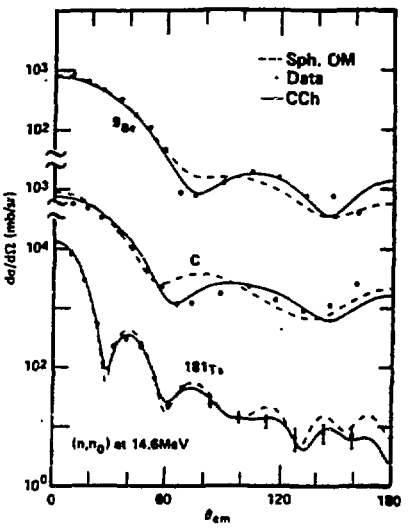

FIG. 8 Measurements of (n,n_o) at 14.6 MeV and OM calculations with deformed (-) and spherical (---) potentials.

Actinide Targets. The ^{232}Th, ^{238}U, and ^{239}Pu(n,n) elastic angular distributions were measured at 14.1 MeV and CC calculations were done for both, microscopic and phenomenological OP. Levels of the GS rotational band up to the 6^+ for Th and U and up to the $9/2^+$ for Pu were included in all the calculations. In the microscopic calculations[7] the real and imaginary terms of the OP were calculated by folding the JLM effective interaction with the deformed GS nuclear density (Legendre polynomial expansion up to $l_{max} = 8$). The spin orbit potential (real) was not deformed and is equal to 45 MeV-fm^5. Fig. 9 shows the results of this calculation (solid line) for ^{238}U. As in the case of Ta, the plotted curves correspond to the sum of the GS and excited levels

differential cross sections. The values of the normalizing parameters λ_R and λ_W for the three nuclei were 0.94 and 0.82 respectively. This calculation has in addition to the normalizing parameters already described for the MOP for the spherical nuclei, the parameters for the ranges of the real (1.2 fm) and imaginary (1.3 fm) parts of the effective interaction (details are found in Ref. 5). The dashed curve corresponds to calculations with the global OP of Klepatskij et al.[6]. This calculation gives a representation of the data comparable with the one obtained from the global potential, although both results could be improved by a better representation of the spin orbit potential.

PROTON OPTICAL POTENTIALS AND THE LANE FORMALISM

The validity of the Lane model[11] in the actinide region was tested by solving the Lane CC equations for the proton and neutron channels [(p,p) and $(p,n)_{IAS}$] in order to extract the (n,n) cross sections. Because of the energy resolution of the measurements and the intrinsic width of the analog state, 250 keV, the Lane equations were generalized[13] to include couplings to the low excited states of the target and their analogs. Since the Coulomb displacement energy for these nuclei is 20-21 MeV, the proton optical model parameters were taken from a CC analysis[14] for 35 MeV protons scattered from ^{232}Th and ^{238}U. The value of the isovector potential V_1 was taken from the analysis of $(p,n)_{IAS}$ measurements at 26 MeV (see Ref. 13 for details).

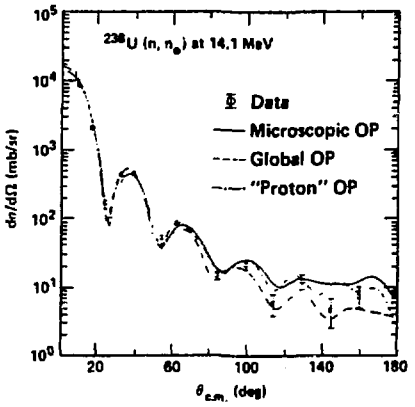

FIG. 9 Measured $^{238}U(n,n_o)$ at 14.1 MeV and calculations with deformed optical potentials: JLM(-), global (---_, "Proton" (-.-).

The predicted angular distribution for the scattered neutrons (sum of GS + excited levels) at 14 MeV is shown in Fig. 9 by the dash-dotted curve. The result compares quite well with those obtained with the microscopic and global potentials for neutron scattering. Calculations with the above potentials, MOP, global, and "Proton" potentials were also carried out for ^{232}Th and ^{239}Pu. The results were quite similar to those obtained for U and are not shown.

CONCLUSIONS

Measurements of neutron and proton angular distributions over a wide mass range (^{9}Be to ^{239}Pu) and energy range (8-65 MeV) have been compared with optical model calculations for two microscopic potentials (MOP), the JeuKenne, Lejeune, and Mahaux (JLM), and the Brieva and Rook (BR) potentials. The comparison with the data has been done using only two free parameters λ_V and λ_W which account for the adjustment of the strengths of the real and imaginary parts respectively of the central potential. The test[3] of these MOP over a mass range was done using the new measurements at 14.6 MeV for targets ranging from Be to Bi. The test[8] over energy range has been done for some light nuclei (C, O, N, Al), and for ^{54,56}Fe and ^{208}Pb. The results of these comparisons are: 1) The agreement with the data is reasonably good, with the JLM potential giving consistently better results than the BR. 2). The normalizing parameter λ_V is within a few percent of unity for all cases. 3) λ_W exibits a mass and energy variation which is most pronounced for the BR potential. 4) The results obtained with the JLM potential at 14.6 MeV compare well with those obtained with phenomenological potentials[4] optimized over the mass region. 5) The neutron scattering calculations are not sensitive to an increase in the neutron rms radius relative to that for the protons (neutron skin) in the energy range of these measurements (8-26 MeV). 6) The proton scattering calculations (20-65 MeV) are sensitive to the inclusion of a neutron skin, which improve the fits to the data.

The neutron angular distributions at 14.6 MeV from deformed nuclei (Be, C, Ta, ^{232}Th, ^{238}U, and ^{239}Pu) were also analyzed using coupled channel (CC) calculations and deformed optical potentials[6,17], with noticeable improvement in the agreement with the data. In addition, the analysis of the neutron data from the actinide targets was also compared with CC using the Lane formalism with deformed proton potentials. These results compare quite well with those obtained with the microscopic and global optical potentials.

The understanding of microscopic optical potentials and their value as a tool to predict neutron differentical cross sections will benefit from neutron measurements at higher energies (E > 30 MeV). The energy dependence of the effective interaction, the Coulomb correction to the absorption potential, details of the isovector potential need to be tested against the combined analysis of neutron and proton measurements in the same energy range. Furthermore, evaluations of neutron libraries need also to have measurements of cross sections at least up to 40 MeV, in order to test the nuclear models being used in the libraries.

ACKNOWLEDGEMENTS

In the present paper I have summarized work that has been carried out at Livermore and at Ohio University. I would like to thank those who have participated in the different topics discussed here, including F. S. Dietrich, R. Finlay, R. C. Haight, Ch. Lagrange, S. Mellema, F. Petrovich, B. A. Pohl, C. H. Poppe, and C. Wong. This review has been performed under the auspices of the U.S. Department of Energy by the LLNL under contract number W-7405-ENG-48.

REFERENCES

1. J. P. Jeukenne, A. Lejeune, and C. Mahaux, Phys. Rev. C 16, 80 (1977).
2. F. A. Brieva and J. R. Rook, Nucl. Phys. A291, 299 (1977); A291, 317 (1977).
3. L. F. Hansen, F. S. Dietrich, B. A. Pohl, C. H. Poppe, C. Wong, Phys. Rev. C 31, 111 (1985). See Ref. 1-36.
4. J. Rapaport, V. Kulkarni, and R. W. Finlay, Nucl. Phys. A330, 15 (1979).
5. Ch. Lagrange, M. Girod, J. Phys. G: Nucl Phys 9, 197 1983.
6. A. B. Klepatskij, V. A. Kon'shin and E. Sh. Sukhovitskij, "The Optical Potential for Heavy Nuclei," INDC(CCP)-161/L 1980.
7. L. F. Hansen, R. C. Haight, B. A. Pohl, C. Wong, "Neutron-Nucleus Collisions A Probe of Nuclear Structure," AIP 124, Conf. Proc. 314 (1984).
8. F. S. Dietrich and F. Petrovich, AIP 124, 90 (1984).
9. S. Mellema, R. W. Finlay, F. S. Dietrich, Phys. Rev. C 28, 2267 (1983).
10. J. S. Petler, M. S. Islam, R. W. Finlay, F. S. Dietrich, "Microscopic Optical Model Analysis of Nucleon Scattering from Light Nuclei" (unpublished).
11. A. M. Lane, Phys. Rev. Lett. 8, 171 (1962); Nucl. Phys. 35, 676 (1972).
12. L. F. Hansen, Study of Proton-Induced Reactions and Correlations with Fast Neutron Scattering, UCRL-86961.Proc. of the Specialists' Meeting on "Fast Neutron Scattering on Actinide Nuclei", OECDI, OCDE, Paris, Nov. 1981. NEANDC - 158U (See Ref. 46-48).
13. L. F. Hansen, S. M. Grimes, C. H. Poppe, C. Wong, Phys. Rev. C 28, 1934 (1983).
14. R. M. Ronningen, R. C. Melin, J. A. Nolen, G. M. Crawley, Phys. Rev. Lett. 47, 635 (1981).
15. G. Bertsch, J. Borysowicz, H. McManus, W. G. Love, Nucl. Phys. A284, 399 (1977).
16. J. Raynal, The Structure of Nuclei: Trieste Lectures 1971. STI/PUB/305 (Vienna: IAEA), 1972.
17. A. S. Meigooni, J. S. Petler, R. W. Finlay, Phys. Med. Biol., 1984, Vol. 29, 643 (1984).